

Computation of strained epitaxial growth in three dimensions by kinetic Monte Carlo

Giovanni Russo^a, Peter Smereka^{b,*}

^a *Dipartimento di Matematica e Informatica, Università di Catania, Catania, Italy*

^b *Department of Mathematics, University of Michigan and the Michigan Center for Theoretical Physics, 525 E
University Avenue, Ann Arbor, MI 48109-1109, United States*

Received 25 January 2005; received in revised form 9 August 2005; accepted 17 October 2005
Available online 2 December 2005

Abstract

A numerical method for computation of heteroepitaxial growth in the presence of strain is presented. The model used is based on a solid-on-solid model with a cubic lattice. Elastic effects are incorporated using a ball and spring type model. The growing film is evolved using kinetic Monte Carlo (KMC) and it is assumed that the film is in mechanical equilibrium. The force field in the substrate is computed by an exact solution which is efficiently evaluated using the fast Fourier transform, whereas in the growing film it is computed directly. The system of equations for the displacement field is then solved iteratively using the conjugate gradient method. Finally, we introduce various approximations in the implementation of KMC to improve the computation speed. Numerical results show that layer-by-layer growth is unstable if the misfit is large enough resulting in the formation of three dimensional islands.

© 2005 Elsevier Inc. All rights reserved.

Keywords: Epitaxial growth; Strain; Kinetic Monte Carlo

1. Introduction

Epitaxial growth is the process where crystals are grown by the deposition of atoms in a vacuum. Typically, the deposition rate is small and the crystal is grown, loosely speaking, one layer at a time. In this paper, we consider the computation of strained epitaxial growth when the strain arises because the natural lattice spacing of the substrate and the deposited material are different. This difference is called the *misfit*. Heteroepitaxial growth is experimentally observed to grow in the following modes:

1. Frank–Van der Meer growth: crystal surface remains fairly flat, growth occurs in the layer-by-layer fashion.
2. Volmer–Weber growth: three dimensional islands form on the substrate without a wetting layer.

* Corresponding author.

E-mail address: psmereka@umich.edu (P. Smereka).

3. Stranski–Krastanov growth: the film grows in a layer-by-layer fashion for a few layers, and then Volmer–Weber growth begins. This results in three dimensional islands on top of a wetting layer.

The type of growth mode depends on many parameters, an important one is the misfit. In many cases, when the misfit is high, one finds Volmer–Weber growth and when the misfit is small layer-by-layer growth is observed. For intermediate values of the misfit Stranski–Krastanov growth is often seen. For an overview see, for example [22,15].

In homoepitaxy, the effects of strain are usually very small and quite often ignored in the many models. In general, the morphology of a growing film by homoepitaxy is reasonably well understood. It is known that in some cases a homoepitaxially grown film can undergo an instability resulting in mound formation. Typically, these phenomena are due to kinetic effects, for example, a step-edge barrier [2,6,7] or enhanced edge diffusion [16] can cause mound formation.

However, when a species of atoms grows on a substrate of a different species, formation of 3D islands is observed in many situations. It is generally believed in many cases (for example for the growth of germanium on silicon) that this is a thermodynamical effect. In particular, the elastic energy stored in a strained flat interface is greater than when there are three dimensional islands. This is due to the fact that in the latter case the atoms have more opportunity to relax (see Fig. 1). However, the surface energy of three dimensional islands is greater than that of a flat interface. This implies that the morphology of heteroepitaxially grown films is determined by the interplay between elastic energy which is a bulk effect and surface energy which arises from broken bonds.

1.1. Modeling elastic effects

Elastic effects in thin films can be studied with fully continuum models or Burton–Cabrera–Frank [5] type models that consider elastic effects between steps. In this paper, we shall consider a fully discrete model which is evolved in time using a kinetic Monte Carlo method. Naturally, such an approach has the disadvantage of not being able to simulate on large length scales. However, it offers the advantage that nanoscale physical effects such as island shape fluctuations and nucleation are naturally incorporated. One of the first, if not the first, model in this direction is due to Orr et al. [14]. They accounted for the elastic interactions using a ball and spring model, which takes into account nearest neighbor and next nearest neighbor interactions. This was combined with a solid-on-solid type model which was then used with KMC to simulate a growing heteroepitaxial film in $1 + 1$ dimensions. If the misfit was below a critical value, the film grew in a layer-by-layer fashion. On the other hand, if the misfit was above the same critical value, then the film was observed to grow in the Volmer–Weber fashion. Later Lam et al. [8] provided a more efficient implementation of this model, which

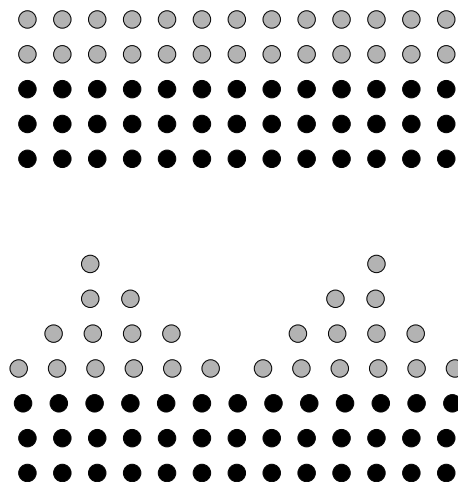


Fig. 1. Germanium on silicon – due to elastic interaction, the bottom configuration has less energy than the top one.

allowed them to perform simulations using parameter values that were more physically reasonable, and to compute for larger domains. This work has been recently extended to three dimensions [9].

Ratsch et al. [19] studied three dimensional heteroepitaxy, however they did not take explicitly into account the harmonic forces between atoms, but rather they used an approximate treatment [18] based on the Frenkel–Kontorova model. The model was used to investigate the island size distribution in heteroepitaxial growth [17].

Off lattice KMC simulations of heteroepitaxial growth in 1 + 1 dimensions were presented in a series of papers [3,10,12]. Prior to this, off lattice KMC had been used to investigate diffusion on strained surfaces [23]. In these computations the forces between atoms were modeled using Lennard–Jones interactions. The misfit is easily incorporated by changing parameters in the potential. One advantage of this approach is that dislocations are naturally included, which is not the case with the ball and spring model. These simulations also demonstrate that if the misfit is sufficiently large, layer-by-layer growth is unstable and mounds form.

A more sophisticated discrete elastic model was introduced by Schindler et al. [21]. This model is based on a discrete form of the continuum elasticity equations. The approach presented here could be used to solve their model as well.

2. Model description and Kinetic Monte Carlo

The model we shall use is a three dimensional version of the one proposed in [8,14]. For the convenience of the reader we shall now describe this model. To fix ideas we shall assume that the deposited atoms are germanium and the substrate is composed of silicon. The atoms occupy sites arranged on a simple cubic lattice with no over hanging atoms allowed. This means that the height of the surface is a function of the two horizontal coordinates. We assume that atoms bond with their nearest and next nearest neighbors. Each atom can be linked to its six nearest neighbors located at a distance a , and to its twelve next neighbors located at a distance $a\sqrt{2}$. For example, a surface atom of a flat plane orthogonal to one of the coordinate axis will have five bonds with nearest neighbors, and eight bonds with next nearest neighbors, while an atom sitting on top of that same flat surface will have five bonds (one with a nearest neighbor and four with next nearest neighbors). We shall assume the chemical energy associated to all these bonds is the same. The total chemical bond energy associated to each atom is therefore $E_b = -\gamma N_b$, where N_b is the number of bonds of each atom, and γ the energy associated to each bond.

The elastic effects in this model are taken into account by assuming that the bonds will act like a spring between the atoms. We will use a_s and a_g to denote the lattice spacing between silicon and germanium atoms, respectively. We shall denote respectively by k_L and k_D the spring constants corresponding to longitudinal (nearest neighbor) and diagonal (next nearest neighbor) bonds. For ease of exposition, we shall assume that both silicon and germanium have the same spring constants. Since $a_g \neq a_s$, mechanical forces will arise (the calculation of which is described in detail below). It will be assumed that our mass-spring system is always in mechanical equilibrium. The time it takes for the system to reach mechanical equilibrium is of the order of the time it takes for sound wave to cross the width of the wafer. Assuming a thickness of 1 μm , this time is about 1 ns. The hopping rate of adatoms on silicon (this is the fastest process we are considering) is of the order of 10^5 – 10^6 hops/s. Since the mechanical relaxation time is much smaller than the inverse of the hopping frequency, the assumption of mechanical equilibrium appears to be a very reasonable approximation.

Each surface atom, p , of the system will hop with a rate R [8] given by

$$R = R_0 \exp\left(\frac{-\delta E}{k_B T}\right), \quad (1)$$

where

$$\delta E = E(\text{without atom } p) - E(\text{with atom } p) \quad (2)$$

is the change in energy of the entire system when atom p is completely removed. R_0 is the attempt frequency, k_B is the Boltzmann constant, and T is the lattice temperature. Since the chemical bonds are purely local, then we can write (2) as

$$\delta E = N_b \gamma - \Delta E_s,$$

where N_b is the number of chemical bonds of the atom, γ is the energy associated to the chemical bond, and

$$\Delta E_s = E_s(\text{with atom } p) - E_s(\text{without atom } p), \quad (3)$$

with E_s denoting the total elastic energy. We note that ΔE_s is almost always positive and when combined with (2) implies that elastic effects will tend to increase the hopping rate.

We shall evolve the model in time by the use of kinetic Monte Carlo (KMC). The basic KMC method can be described as follows. We consider a $M \times M$ lattice with periodic boundary conditions.

1. Every N_{add} steps, pick a surface site at random among the M^2 , and add an atom there.
2. Pick an atom at random on the surface, uniformly among all surface atoms.
3. Compute its number of bonds.
4. Compute the contribution of the elastic energy associated to the atom.
5. Choose a random direction, uniformly among all possible directions, and perform one hop in that direction with probability $P = (R_0/Z) \exp(-(N_b \gamma - \Delta E_s)/k_B T)$, where Z is computed so that $P \leq 1$. This basic KMC algorithm has a time step $\Delta t = 1/Z$. The adatom flux F is given by $F = Z/(M^2 a_s^2 N_{\text{add}})$. Note that after each event, we advance the clock by a fixed amount Δt , rather than by an exponentially distributed time, as it would be more appropriate for a Poisson process. However, this approximation has very little influence on the actual dynamics.

While this model is idealized, it nevertheless captures the essential physical effects of heteroepitaxial growth, such as adatom diffusion, nucleation, surface diffusion, and long range elastic interaction. In addition, since the model is evolved in time using kinetic Monte Carlo, it naturally captures effects associated with fluctuations.

3. Elastic computations

The main difficulty in the implementation of this model is the computation of the strain field. In this section, we shall outline our approach for solving this problem. For the basic set up we follow Lam et al. [8], as described below. However, our numerical implementation is different from the one used in [8]. One important feature of our work is that we provide an exact solution for the elastic displacement in the substrate which is efficiently evaluated using fast Fourier transforms.

3.1. The reference configuration

The reference configuration we choose consists of a periodic array of complete layers of germanium atoms on top of a periodic array of silicon. The germanium atoms are compressed so that their horizontal lattice spacing matches that of the silicon atoms, see Figs. 2 and 3. The vertical lattice spacing, a_L , is chosen so that the resulting system is in mechanical equilibrium. We will now describe the computation of a_L in two dimensions. It is useful to introduce the following dimensionless quantity:

$$\epsilon = \frac{a_g - a_s}{a_s},$$

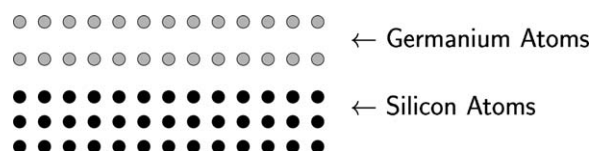


Fig. 2. The reference configuration is obtained by compressing the germanium atoms to have the same horizontal spacing as the silicon atoms. The vertical spacing is chosen so that germanium atoms are in equilibrium.

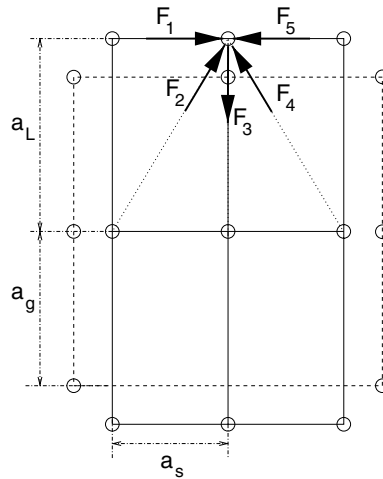


Fig. 3. The reference configuration is obtained by compressing the germanium atoms to have the same horizontal spacing as the silicon atoms. The vertical spacing is chosen so that complete layers of germanium are in equilibrium. \vec{b} is the net force on an atom due to the compression. In principle \vec{b} can be nonzero for any germanium or silicon atoms in the top row, if the top layer is not complete.

which is denoted as the misfit. Typical values of ϵ range from -0.05 to 0.05 . For example the misfit for germanium on a silicon substrate is 0.04 . In order to deduce the atom displacement with respect to the reference configuration we need to compute the forces experienced by an atom due to each of its neighbors. Elementary considerations show, to first order in the ratio ϵ , one has

$$\vec{F}_1 = F_H \begin{pmatrix} 1 \\ 0 \end{pmatrix}, \quad \vec{F}_2 = F_{DV} \begin{pmatrix} 1 \\ 1 \end{pmatrix}, \quad \vec{F}_3 = F_V \begin{pmatrix} 0 \\ -1 \end{pmatrix}, \quad \vec{F}_4 = F_{DV} \begin{pmatrix} -1 \\ 1 \end{pmatrix}, \quad \vec{F}_5 = -\vec{F}_1,$$

where $F_V = k_L(a_L - a_g)$, $F_H = k_L(a_g - a_s)$, and $F_{DV} = k_D(2a_g - a_L - a_s)/2$.

The value of a_L is determined by requiring that these five forces sum to zero for atoms in the reference configuration. By symmetry, the forces in the x direction sum to zero. On the other hand, balancing the z components of the force one has $2F_{DV} = F_V$ which implies

$$k_D(2a_g - a_L - a_s) + k_L(a_g - a_L) = 0,$$

and gives the following expression for a_L

$$a_L = a_g + a_s \epsilon \frac{k_D}{k_L + k_D}.$$

A similar argument can be applied to the three dimensional lattice. In this case each atom can interact with 6 nearest neighbors, located at a distance a , and 12 diagonal next to nearest neighbors, located at distance $a\sqrt{2}$. The interaction with the 8 corner neighbors, located at a distance $a\sqrt{3}$, is neglected.

As in the two dimensional case, we shall denote by k_L and k_D the two spring constants corresponding to the interaction between nearest neighbors and diagonal neighbors. Each bulk atom is surrounded by 18 neighbors (6 longitudinal and 12 diagonal). We denote by $\vec{F}_{\ell jk}$ the contribution of the force on a given atom due to the presence of its neighbor in the direction (ℓ, j, k) . For example, the 3D equivalent of force \vec{F}_3 of Fig. 3 would be $\vec{F}_{0,0,-1}$.

The six forces aligned along the coordinate axis have the expression

$$\vec{F}_{\ell jk} = \begin{pmatrix} -\ell F_H \\ -j F_H \\ k F_V \end{pmatrix}, \quad \text{with } \ell, j, k \in \{-1, 0, 1\}, \quad \text{where } |\ell| + |j| + |k| = 1. \tag{4}$$

F_V and F_H are given above. The 12 diagonal forces are given by

$$\vec{F}_{\ell 0k} = - \begin{pmatrix} \ell F_{DV} \\ 0 \\ k F_{DV} \end{pmatrix}, \quad \text{with } \ell, k \in \{-1, 1\}, \quad (5)$$

$$\vec{F}_{0jk} = - \begin{pmatrix} 0 \\ j F_{DV} \\ k F_{DV} \end{pmatrix}, \quad \text{with } j, k \in \{-1, 1\}, \quad (6)$$

and

$$\vec{F}_{\ell j0} = - \begin{pmatrix} \ell F_{DH} \\ j F_{DH} \\ 0 \end{pmatrix}, \quad \text{with } \ell, j \in \{-1, 1\}, \quad (7)$$

F_{DV} is given above and $F_{DH} = k_D(a_g - a_s)$. It is convenient to set $\vec{F}_{\ell jk} = 0$ if $|\ell| + |j| + |k| = 3$.

As in the two dimensional case these forces must sum to zero in the reference configuration. The x and y components will vanish by symmetry. The forces in the z direction vanish if

$$F_V - 4F_{DV} = 0,$$

which implies

$$2k_D(2a_g - a_L - a_s) + k_L(a_g - a_L) = 0.$$

This gives the following expression:

$$a_L = a_g + a_s \epsilon \frac{2k_D}{k_L + 2k_D}. \quad (8)$$

It follows from (8) that the forces given by Eqs. (5)–(7) are antisymmetric with respect to ϵ . As we shall see, this means that switching sign of ϵ switches the sign of the displacement field, which in turn does not change the value of the elastic energy (see Section 4). This implies that interface morphologies will only depend on the magnitude of ϵ and not its sign.

3.2. Computation of the interaction

Let us denote the displacement, with respect to the reference configuration, of an atom at site (ℓ, j, k) by the vector $(u_{\ell jk}, v_{\ell jk}, w_{\ell jk})$ and the force experienced by this atom as $(f_{\ell jk}, g_{\ell jk}, h_{\ell jk})$. This force will arise from the interaction of the atom with its nearest neighbors and next nearest neighbors. For example the x component of the force is given by

$$\begin{aligned} f_{\ell jk} = & k_L([u_{\ell+1jk} - u_{\ell jk}] + [u_{\ell-1jk} - u_{\ell jk}]) + \frac{k_D}{2}([u_{\ell+1jk+1} - u_{\ell jk}] + [u_{\ell-1jk+1} - u_{\ell jk}]) \\ & + \frac{k_D}{2}([u_{\ell+1jk-1} - u_{\ell jk}] + [u_{\ell-1jk-1} - u_{\ell jk}]) + \frac{k_D}{2}([u_{\ell+1j+1k} - u_{\ell jk}] + [u_{\ell-1j+1k} - u_{\ell jk}]) \\ & + \frac{k_D}{2}([u_{\ell+1j-1k} - u_{\ell jk}] + [u_{\ell-1j-1k} - u_{\ell jk}]) + \frac{k_D}{2}([v_{\ell+1j+1k} - v_{\ell jk}] + [v_{\ell-1j-1k} - v_{\ell jk}]) \\ & - \frac{k_D}{2}([v_{\ell+1j-1k} - v_{\ell jk}] + [v_{\ell-1j+1k} - v_{\ell jk}]) + \frac{k_D}{2}([w_{\ell+1jk+1} - w_{\ell jk}] + [w_{\ell-1jk-1} - w_{\ell jk}]) \\ & - \frac{k_D}{2}([w_{\ell+1jk-1} - w_{\ell jk}] + [w_{\ell-1jk+1} - w_{\ell jk}]) + \sum_{(m,n,q) \in \text{neigh}(\ell,j,k)} \vec{F}_{mnq} \cdot \mathbf{e}_x, \end{aligned} \quad (9)$$

where \vec{F}_{mnq} are given by Eqs. (4)–(7). Each term in square brackets and each \vec{F}_{mnq} represents the interaction of an atom at site (ℓ, j, k) with potential nearest and next nearest neighbors. If no such neighbor exists then the term should not be included.

Suppose we have N atoms and we denote the relative displacement of the p th atom by \vec{u}_p and let \vec{f}_p denote the force it experiences. We also let \vec{b}_p denote the sum of all forces given by Eqs. (4)–(7), acting on the atom when its position is the reference configuration. Next we define the following vectors in \mathbb{R}^{3N} : $\mathbf{u} = (\vec{u}_1, \dots, \vec{u}_N)^T$, $\mathbf{b} = (\vec{b}_1, \dots, \vec{b}_N)^T$ and $\mathbf{f} = (\vec{f}_1, \dots, \vec{f}_N)^T$. Then we can write

$$\mathbf{f} = \mathcal{A}\mathbf{u} + \mathbf{b},$$

since the force depends linearly on the displacement, and \mathbf{b} denotes the force on the atoms when they are in the reference configuration. We remark that for atoms that are completely surrounded by other 18 atoms, or atoms that are on a horizontal surface, the corresponding \vec{b} is zero, since all the forces acting on them sum up to zero, which is consistent to the fact that a rectangular box of atoms in the reference configuration is in equilibrium. As a consequence, the vector \mathbf{b} has nonzero elements only for atoms at the surface. The matrix vector product, $\mathcal{A}\mathbf{u}$, can be deduced from (9) and similar relations for $g_{\ell jk}$ and $h_{\ell jk}$.

The equilibrium position of atoms in a given configuration is obtained by setting $\mathbf{f} = 0$, i.e., by solving the large linear system

$$\mathcal{A}\mathbf{u} + \mathbf{b} = 0.$$

3.3. Contribution of the substrate

It is known that the effect of elastic interactions can be very long ranged. For example, according to Rickman and Srolovitz [20], the elastic interaction between two island behaves like d^{-2} where d is the distance between the island centers. Furthermore, the solution of the Laplace equation on the semi-infinite space with periodic data on the boundary plane, and which decays at infinity, has an exponential decaying rate (see Section 3.3.2). This indicates that elastic interaction can penetrate deep into the substrate. On the other hand, the interaction range is certainly much shorter than the thickness of the substrate. For this reason, it is prudent to consider the substrate to be semi-infinite in the z -direction. To reduce boundary effects we consider periodic boundary conditions in both the x and y directions. In this section, we shall derive a formula that expresses the force on the surface atoms of the substrate completely in terms of their displacement.

The surface of the substrate corresponds to $k = 0$, and the atoms of the bulk substrate will be indexed using negative k values. Inside the substrate ($k \leq -1$) all atoms have a complete set of neighbors, consequently we can explicitly write the force, in component form, on the atom at site (ℓ, j, k) , $k \leq -1$, as function of the displacement of the atom and its neighbors. We shall denote the components of the force by $(f_{\ell jk}, g_{\ell jk}, h_{\ell jk})$. The explicit expression of such forces is given in Eqs. (30)–(32).

At the surface of the substrate ($k = 0$), the expression of the force acting on each silicon atom, due to the presence of the other silicon atoms, is slightly different, since there are no atoms on top. Its explicit expression is reported in Eqs. (33)–(35).

Let us now consider a Fourier expansion of the displacement in the x and y directions. The generic Fourier mode will take the form

$$\begin{aligned} u_{\ell jk} &= \hat{u}_k(\xi, \eta) e^{i(\ell\xi + j\eta)}, \\ v_{\ell jk} &= \hat{v}_k(\xi, \eta) e^{i(\ell\xi + j\eta)}, \\ w_{\ell jk} &= \hat{w}_k(\xi, \eta) e^{i(\ell\xi + j\eta)}. \end{aligned} \tag{10}$$

By inserting this Fourier expansion in the expression of the surface force (33)–(35) one obtains the relations

$$\begin{aligned} \hat{f}_0 &= 2k_L \hat{u}_0 (\cos \xi - 1) + k_D [\hat{u}_{-1} \cos \xi + \hat{u}_0 (2 \cos \xi \cos \eta - 3) - 2\hat{v}_0 \sin \xi \sin \eta - i\hat{w}_{-1} \sin \xi], \\ \hat{g}_0 &= 2k_L \hat{v}_0 (\cos \eta - 1) + k_D [\hat{v}_{-1} \cos \eta + \hat{v}_0 (2 \cos \xi \cos \eta - 3) - 2\hat{u}_0 \sin \xi \sin \eta - i\hat{w}_{-1} \sin \eta], \\ \hat{h}_0 &= k_L (\hat{w}_{-1} - \hat{w}_0) + k_D [\hat{w}_{-1} (\cos \xi + \cos \eta) - 2\hat{w}_0] - i(\hat{u}_{-1} \sin \xi + \hat{v}_{-1} \sin \eta). \end{aligned} \tag{11}$$

In the relation above we have omitted to indicate the dependence of all Fourier modes on (ξ, η) .

Eq. (11) gives a relation between the Fourier modes of the force and the Fourier modes of the displacement. Our goal is to express $(\hat{f}_0, \hat{g}_0, \hat{h}_0)$ in terms of $(\hat{u}_0, \hat{v}_0, \hat{w}_0)$. Once this is done then the force field at the surface can

be computed from its Fourier modes by inverse discrete Fourier transform. In order to accomplish this goal, we need to express $\hat{u}_{-1}, \hat{v}_{-1}, \hat{w}_{-1}$ in terms of $\hat{u}_0, \hat{v}_0, \hat{w}_0$, and substitute their expression into (11). This can be done as follows. First, let us insert the Fourier expansion (10) into Eqs. (30)–(32) obtaining:

$$\begin{aligned}\hat{f}_k &= 2k_L \hat{u}_k (\cos \xi - 1) + k_D [(\hat{u}_{k+1} + \hat{u}_{k-1}) \cos \xi + \hat{u}_k (2 \cos \eta \cos \xi - 4)] \\ &\quad + ik_D (\hat{w}_{k+1} - \hat{w}_{k-1}) \sin \xi - 2k_D \hat{v}_k \sin \xi \sin \eta, \\ \hat{g}_k &= 2k_L \hat{v}_k (\cos \eta - 1) + k_D [(\hat{v}_{k+1} + \hat{v}_{k-1}) \cos \eta + \hat{v}_k (2 \cos \eta \cos \xi - 4)] \\ &\quad + ik_D (\hat{w}_{k+1} - \hat{w}_{k-1}) \sin \eta - 2k_D \hat{u}_k \sin \xi \sin \eta, \\ \hat{h}_k &= k_L (\hat{w}_{k+1} - 2\hat{w}_k + \hat{w}_{k-1}) + k_D [(\hat{w}_{k+1} + \hat{w}_{k-1}) (\cos \xi + \cos \eta) - 4\hat{w}_k] \\ &\quad + ik_D [(\hat{u}_{k+1} - \hat{u}_{k-1}) \sin \xi + (\hat{v}_{k+1} - \hat{v}_{k-1}) \sin \eta].\end{aligned}\tag{12}$$

The discrete equations given by (12) are solved using the following substitution:

$$\hat{u}_k = \hat{u} \alpha^k, \quad \hat{v}_k = \hat{v} \alpha^k, \quad \hat{w}_k = \hat{w} \alpha^k,\tag{13}$$

where we look for solutions with $|\alpha| > 1$, since we expect the Fourier modes to decay as $k \rightarrow -\infty$. Inserting this ansatz into the expression (12) of the Fourier modes of the force acting on the inner points of the substrate, one obtains:

$$\begin{pmatrix} \hat{f} \\ \hat{g} \\ \hat{h} \end{pmatrix} = \Omega(\alpha) \begin{pmatrix} \hat{u} \\ \hat{v} \\ \hat{w} \end{pmatrix},\tag{14}$$

where the entries of the matrix Ω are given by

$$\begin{aligned}\omega_{11} &= 2k_L (\cos \xi - 1) \alpha + k_D [\cos \xi (1 + \alpha^2) + 2(\cos \eta \cos \xi - 2) \alpha], \\ \omega_{22} &= 2k_L (\cos \eta - 1) \alpha + k_D [\cos \eta (1 + \alpha^2) + 2(\cos \eta \cos \xi - 2) \alpha], \\ \omega_{33} &= k_L (\alpha^2 - 2\alpha + 1) + k_D [(\alpha^2 + 1) (\cos \xi + \cos \eta) - 4], \\ \omega_{12} &= \omega_{21} = -2\alpha k_D \sin \xi \sin \eta, \\ \omega_{13} &= \omega_{31} = ik_D (\alpha^2 - 1) \sin \xi, \\ \omega_{23} &= \omega_{32} = ik_D (\alpha^2 - 1) \sin \eta.\end{aligned}$$

Note that matrix Ω is symmetric, but not self-adjoint. Such problems are sometimes referred as *palindromic* equations, because of their symmetric structure, and appear when looking for vibrational modes of three dimensional elastic structures [11].

Since all forces in the bulk have to be zero (all such atoms are in mechanical equilibrium), then one has

$$\Omega \begin{pmatrix} \hat{u} \\ \hat{v} \\ \hat{w} \end{pmatrix} = 0.\tag{15}$$

This homogeneous system has nontrivial solutions only if

$$P(\alpha) \equiv \det(\Omega) = 0.\tag{16}$$

This relation results in an algebraic equation for the values of α . The polynomial $P(\alpha)$ is of degree six, therefore it admits, in general, six roots. Note that, because of the structure of the matrix Ω , matrix $\alpha^2 \Omega(1/\alpha)$ is equal to $\Omega(\alpha)$ with $\omega_{13} = \omega_{31}$ and $\omega_{23} = \omega_{32}$ of opposite sign. This does not change the expression of the determinant, and therefore if $\tilde{\alpha} \neq 0$ is a root, then also $1/\tilde{\alpha}$ is a root. This means that the number of roots $\tilde{\alpha}$ such that $|\tilde{\alpha}| > 1$

is equal to the number of (nonzero) roots $\tilde{\alpha}$ such that $|\tilde{\alpha}| < 1$. The roots that are of interest for us are the ones that decay as $k \rightarrow -\infty$, i.e., $\tilde{\alpha}$: $|\tilde{\alpha}| > 1$.

3.3.1. Eigenvector computation

In this subsection, we describe a general procedure for the computation of the eigenvalues and eigenvectors, that works also in the case of multiple eigenvalues.

The goal is to solve the problem given by (15), which we write as

$$\Omega r = 0, \tag{17}$$

where r is a three-component vector (we drop the arrow on top), and to find independent eigenvectors even if some eigenvalues coincide. First compute the eigenvalues by solving the algebraic equation (16). Consider the three eigenvalues α_ℓ such that $|\alpha_\ell| > 1$, $\ell = 1, \dots, 3$. If they are all distinct, then the three eigenvectors corresponding to them will be independent. If two of them are coincident, let us say $\alpha_2 = \alpha_3$, then one has to find two independent eigenvectors corresponding to the coincident eigenvalues.

A unified treatment of the problem is obtained by the use of the singular value decomposition (SVD) of matrix Ω . The procedure works as follows. First compute $\alpha_1, \alpha_2, \alpha_3$. If they are distinct, for each of them compute $\Omega_\ell = \Omega(\alpha_\ell)$, $\ell = 1, \dots, 3$. Perform the SVD of Ω_ℓ : $\Omega_\ell = U\Sigma V^\dagger$, where U and V are unitary matrices (i.e., $UU^\dagger = I$, $VV^\dagger = I$), and Σ is a diagonal matrix containing the singular values of Ω_ℓ . Taking into account that U is nonsingular, problem (17) reads

$$\Sigma V^\dagger r = 0.$$

Since Ω_ℓ is singular, then $\Sigma = \text{diag}(\sigma_1, \sigma_2, 0)$, therefore one has

$$\sigma_1(V^\dagger r)_1 = 0, \quad \sigma_2(V^\dagger r)_2 = 0, \quad (V^\dagger r)_3 = \text{arbitrary}.$$

Let us choose $(V^\dagger r)_3 = 1$.

Assuming $\sigma_2 \neq 0$, i.e., that the matrix Σ_ℓ has rank 2, then one has

$$V^\dagger r = \begin{pmatrix} 0 \\ 0 \\ 1 \end{pmatrix},$$

therefore

$$r = V \begin{pmatrix} 0 \\ 0 \\ 1 \end{pmatrix},$$

i.e., r is the third column of V .

If two roots are coincident, say $\alpha_1, \alpha_2 = \alpha_3$, then first compute the eigenvector r_1 using the procedure above applied to matrix $\Omega(\alpha_1)$. For the computation of the other eigenvectors there are two possibilities: either the rank of the matrix $\Omega_2 = \Omega_3$ is 1, i.e., $\sigma_2 = 0$, or the rank of the matrix is 2, i.e., $\sigma_2 \neq 0$. However, the latter case never happened in all our computations, and we conjecture it can never happen for our problem. Therefore, we assume that $\sigma_2 = 0$. Repeating the procedure above, one finds that r_2 and r_3 can be computed, respectively, as the second and third column of the matrix V .

3.3.2. Surface force formula

We denote by \vec{r}_ℓ a solution of the system

$$\Omega(\alpha_\ell)\vec{r} = 0,$$

with $\ell = 1, 2, 3$. Then we can decompose the vector $(\hat{u}_0, \hat{v}_0, \hat{w}_0)^\top$ on the basis of the eigenvectors, i.e.

$$\begin{pmatrix} \hat{u}_0 \\ \hat{v}_0 \\ \hat{w}_0 \end{pmatrix} = c_1\vec{r}_1 + c_2\vec{r}_2 + c_3\vec{r}_3. \tag{18}$$

Once the constants c_1, c_2, c_3 are computed, one can write

$$\begin{pmatrix} \hat{u}_{-1} \\ \hat{v}_{-1} \\ \hat{w}_{-1} \end{pmatrix} = \frac{c_1}{\alpha_1} \vec{r}_1 + \frac{c_2}{\alpha_2} \vec{r}_2 + \frac{c_3}{\alpha_3} \vec{r}_3. \quad (19)$$

The two relations allow to express $\hat{u}_{-1}, \hat{v}_{-1}, \hat{w}_{-1}$ in terms of $\hat{u}_0, \hat{v}_0, \hat{w}_0$. Once this is done, one can substitute this expression into (11) and obtain the final relation between $(\hat{f}_0, \hat{g}_0, \hat{h}_0)$ and $(\hat{u}_0, \hat{v}_0, \hat{w}_0)$. This relation has to be computed for all Fourier modes (ξ, η) . Periodicity implies that $\xi = 2\pi m/M, \eta = 2\pi n/M, m, n = 1, \dots, M$.

The complete algorithm for the computation of $\vec{f}_{\ell j 0}$ from $\vec{u}_{\ell j 0}$ can be summarized as follows:

Computation of $\vec{f}_{\ell j 0}$ from $\vec{u}_{\ell j 0}$

0. *Preprocessing.* Given M , for each mode $(m_1, m_2), m_1, m_2 = 1, \dots, M$, solve the eigenvalue problem (15), and store the eigenvalues and eigenvectors.
 1. Given $\vec{u}_{\ell j 0}$, perform the discrete Fourier transform in ℓ and j and compute all Fourier modes $\hat{u}_0, \hat{v}_0, \hat{w}_0$.
 2. For each mode, compute $\hat{u}_{-1}, \hat{v}_{-1}, \hat{w}_{-1}$ using pre-computed values of eigenvalues and eigenvectors, using Eq. (19).
 3. Compute the Fourier modes of the force $\hat{f}, \hat{g}, \hat{h}$, using Eq. (11).
 4. Compute the force by inverse discrete Fourier transform.

All discrete Fourier transforms can be efficiently computed by FFT algorithms in $O(M^2 \log M)$ operations. In all our calculations we used the FFTW package developed at MIT [1]. It is natural to ask what is the computational cost for a direct evaluation of $\vec{f}_{\ell j 0}$ which does not make use of a FFT algorithm. Since the interaction is only between nearest and next nearest neighbors then the cost will be $O(HM^2)$ where H is the thickness of the substrate, chosen to be sufficiently large so as to model an infinite substrate. To estimate how large one needs to choose H we can appeal to the results in 3.3. The Fourier modes calculated in 3.3 all decay exponentially fast, the slowest one is given by the smallest value of $\alpha : |\alpha| > 1$, denoted α_{\min} . A numerical computation shows that

$$\alpha_{\min} \approx 1 + \frac{C}{M},$$

where $C \approx 3.6$. If we wish that this mode has decayed to $\delta \ll 1$ then the substrate thickness, H , is

$$H \approx \frac{M \log(1/\delta)}{C}.$$

For example if $\delta = 10^{-4}$ then $H \approx 2.5M$. Therefore, the computational cost of computing directly is $\vec{f}_{\ell j 0}$ is $O(M^3 \log \delta^{-1})$, where δ is the required tolerance in the slowest decaying Fourier mode.

3.4. Elastic displacement computation

Let us assume that we have deposited N atoms on a substrate of size $M \times M$. Since we are using a solid-on-solid model, the height of the film is a function of the horizontal lattice location (i, j) . Given the height, the location of all the germanium atoms is then determined. For each germanium atom we make a list of nearest and next nearest neighbors. This list is used to ascertain the interaction forces experienced by germanium atoms. Let us use $\mathbf{u}_g \in \mathbb{R}^{3N}$ to denote the relative displacement of the germanium atoms. We use $\mathbf{u}_s \in \mathbb{R}^{3M^2}$ to denote the relative displacement of the top layer of atoms of the substrate.

The equilibrium position of the particles can be obtained by solving the following linear system

$$\mathbf{F} \equiv \begin{pmatrix} \mathbf{f}_s \\ \mathbf{f}_g \end{pmatrix} = \begin{pmatrix} S & B \\ B^T & A \end{pmatrix} \begin{pmatrix} \mathbf{u}_s \\ \mathbf{u}_g \end{pmatrix} + \begin{pmatrix} \mathbf{b}_s \\ \mathbf{b}_g \end{pmatrix} = 0. \quad (20)$$

The matrices appearing in the system have the following meaning. The forces acting on the M^2 silicon atoms on the surface of the substrate are

$$\mathbf{f}_s = \mathbf{S}\mathbf{u}_s + \mathbf{B}\mathbf{u}_g + \mathbf{b}_s.$$

Here $\mathbf{S}\mathbf{u}_s$ is the force on the atoms at the surface of the substrate due to *all* the (silicon) atoms in the substrate. This is efficiently computed using the results from the previous section. $\mathbf{B}\mathbf{u}_g$ is the force on the substrate surface due to the germanium atoms, and \mathbf{b}_s is the sum of the forces given by (4)–(7). The force acting on the N germanium atoms on the substrate is given by

$$\mathbf{f}_g = \mathbf{B}^T\mathbf{u}_s + \mathbf{A}\mathbf{u}_g + \mathbf{b}_g,$$

where $\mathbf{A}\mathbf{u}_g$ are the forces that arise from the interactions between the germanium atoms, $\mathbf{B}^T\mathbf{u}_s$ is the force on the germanium atoms due to the top layer of silicon atoms, and \mathbf{b}_g is the sum of the forces given by (4)–(7).

We observe that the matrix

$$\begin{pmatrix} S & B \\ B^T & A \end{pmatrix} \tag{21}$$

is a symmetric negative semi-definite matrix; it has three zero eigenvalues, corresponding to the free translation in the three directions of the coordinate axis. The system is clearly invariant for translation along the directions parallel to the substrate. It is also invariant along the direction orthogonal to the substrate, because the substrate is considered semi-infinite. This can be understood by the following argument. For a substrate of a finite thickness, let us say of N_L layers, a unit displacement in the direction orthogonal to the substrate will produce an elastic force per unit atom equal to

$$f = \frac{1}{N_L}(k_L + 2k_D),$$

which vanishes as $N_L \rightarrow \infty$. Therefore, no resistance is opposed to any translation.

Notice that the matrix \mathbf{B}^T is the transpose of matrix $\mathbf{B} \in \mathbb{R}^{3M^2 \times 3N}$. \mathbf{A} is a $3N \times 3N$ matrix. \mathbf{A} and \mathbf{B} are sparse and the matrix vector products are efficiently evaluated using expressions similar to (9). This is done by using the neighbor lists constructed from the height profile.

System (20) can be solved by an iterative scheme for large, sparse linear systems, making use of the symmetry and definiteness of the coefficient matrix. Here we shall use the conjugate gradient method, leaving the search for a more efficient method to future investigations.

4. Evaluation of the elastic energy

Once the strain field is determined, the elastic energy is computed as follows. The energy associated to the bonds is given by

$$E_s = E_{\text{Ge-Ge}} + E_{\text{Ge-Si}} + E_{\text{Si-Si}},$$

where $E_{\text{Si-Si}}$ is the energy due to the interaction between the silicon atoms. The other terms are analogously defined. One has

$$E_{\text{Si-Si}} = \sum_{\text{Si-Si bonds}} \frac{1}{2} k_{\text{bond}} (\ell_{\text{bond}})^2, \tag{22}$$

where k_{bond} is either k_L or k_D depending on whether the bond is longitudinal or diagonal. ℓ_{bond} is the amount the bond has been stretched from the equilibrium configuration. This can be written in terms of the displacement field as

$$E_{\text{Si-Si}} = -\frac{1}{2} \mathbf{u}_{\text{Si}}^T \mathbf{A}_{\text{Si}} \mathbf{u}_{\text{Si}}, \tag{23}$$

where we denote by \mathbf{A}_{Si} the (infinite dimensional) matrix that provides the force on all silicon atoms as a function of the position of the silicon atoms.

The energy due to the interaction of the germanium atoms can be written as

$$E_{\text{Ge-Ge}} + E_{\text{Ge-Si}} = \sum_{\text{all Ge bonds}} \frac{1}{2} k_{\text{bond}} (\ell_{\text{bond}})^2, \quad (24)$$

where k_{bond} is as in (22) but here ℓ_{bond} represents the amount the germanium bonds have been stretched from their original equilibrium configuration (as opposed to the reference configuration). This can be written as

$$E_{\text{Ge-Ge}} + E_{\text{Ge-Si}} = \frac{1}{2} \sum_{\text{all atoms bonded to a Ge atom}} e_{\ell jk}, \quad (25)$$

where $e_{\ell jk}$ is the total elastic energy stored in all the bonds associated to the atom located at site (ℓ, j, k) . The factor $\frac{1}{2}$ accounts for the double counting of the summation. We can write

$$e_{\ell jk} = e_{\ell jk}^x + e_{\ell jk}^y + e_{\ell jk}^z$$

with

$$\begin{aligned} e_{\ell jk}^x &= \frac{k_L}{2} ([u_{\ell+1jk} - u_{\ell jk} + d_x]^2 + [u_{\ell-1jk} - u_{\ell jk} - d_x]^2) + \frac{k_D}{2} ([u_{\ell+1jk+1} - u_{\ell jk} + d_x]^2 + [u_{\ell-1jk+1} - u_{\ell jk} - d_x]^2) \\ &\quad + \frac{k_D}{2} ([u_{\ell+1jk-1} - u_{\ell jk} + d_x]^2 + [u_{\ell-1jk-1} - u_{\ell jk} - d_x]^2) + \frac{k_D}{2} ([u_{\ell+1j+1k} - u_{\ell jk} + d_x]^2 + [u_{\ell-1j+1k} - u_{\ell jk} - d_x]^2) \\ &\quad + \frac{k_D}{2} ([u_{\ell+1j-1k} - u_{\ell jk} + d_x]^2 + [u_{\ell-1j-1k} - u_{\ell jk} - d_x]^2), \end{aligned}$$

where $d_x = a_s - a_g$. In the above expression, each term in square brackets represents the contribution to the elastic energy by a pair of atoms. If no such pair exists then the term is not included. One can derive analogous expressions for $e_{\ell jk}^y$ and $e_{\ell jk}^z$ where $d_y = d_x$ and $d_z = a_L - a_g$.

To compute the total elastic energy, the sum in Eq. (24) is computed directly, while the sum in Eq. (22), which contains infinitely many terms, can be computed by the following argument. First, let us distinguish between the surface and the bulk atoms. Let us denote by $-\mathbf{F}_{\text{Si}}$ the force acting on silicon due to the presence of the germanium. They take the form

$$\mathbf{F}_{\text{Si}} = \begin{pmatrix} \mathbf{F}_s \\ 0 \end{pmatrix},$$

where the dimension of the vector \mathbf{F}_s is equal to $3M^2$, while the force acting on rest of all the infinite atoms of the substrate is zero.

At equilibrium, the net force acting on all silicon atoms is zero, therefore we may write

$$-\mathbf{F}_{\text{Si}} + A_{\text{Si}} \begin{pmatrix} \mathbf{u}_s \\ \mathbf{u}_{\text{bulk}} \end{pmatrix} = 0.$$

Using the above relations one obtains

$$E_{\text{Si-Si}} = -\frac{1}{2} \begin{pmatrix} \mathbf{u}_s \\ \mathbf{u}_{\text{bulk}} \end{pmatrix}^T \begin{pmatrix} \mathbf{F}_s \\ 0 \end{pmatrix} = -\frac{1}{2} \mathbf{u}_s^T \mathbf{F}_s.$$

We remark here that \mathbf{F}_s is the same surface force computed in the previous section using the discrete Fourier transform.

5. Time stepping approximations

The method outlined in Section 2 is impractically slow for the following reasons:

1. For each attempted hop, a complete elastic computation has to be performed. Since most attempts are rejected, most of the time would be spent performing elastic computations that are never used.
2. Even without elastic effects, the simple rejection-based KMC described here is very slow. A more effective technique would be to use rejection-free KMC, in which all possible events are sampled according to their probability [4,13]. However, with the inclusion of elastic effects, the implementation of rejection-free KMC is not so straightforward.
3. Although unlikely, a silicon atom could jump off the substrate and start hopping, and a germanium atom could occupy its previously occupied site. This could result in a mixing between silicon and germanium. Within the present model, we neglect this effect, which may turn out to be important in some situations.

Here we shall outline various approximations of the model which lead to a much faster code, without significantly compromising the physical fidelity.

As mentioned above, in order to know the rate at which an atom might hop we must compute the change in elastic energy of the entire system with and without that atom present. We make the following approximation, we assume that the change in the elastic energy is due to the energy in the bonds that directly connect that atom. Therefore, we have

$$\Delta E_s \approx \sum_{\text{bonds to atom } p} \frac{k_{\text{bond}}}{2} (\ell_{\text{bond}})^2 = e_{\ell j k}, \quad (26)$$

where (ℓ, j, k) is the site of the p th atom. The advantage of this approach is that a new equilibrium configuration has to be computed only if the move is accepted. Another approximation involves updating the displacement field after a given number of hops, denoted as J .

Next, we consider adatom motion. In principle, one should compute its elastic energy which determines its hopping rate; instead we shall assume that the hopping rate of adatoms is the same as it would be on an infinite substrate. This rate can be easily estimated numerically by computing the displacement field for single adatom on a substrate and then using (26). In this way, the hopping rate for adatom is given by:

$$R_5 = R_0 \exp((-5\gamma + \Delta E_0)/k_B T), \quad (27)$$

where $-5\gamma + \Delta E_0$ is the energy required to completely remove an adatom from an empty substrate, and ΔE_0 is the elastic energy associated with a single atom on top of a flat substrate (estimated using Eq. (26)). The reader is reminded that the 5 is present since usually an adatom has at least 5 bonds. Although adatoms with less than 5 bonds will hop at higher rate we assume that they hop at the same rate as given above.

It is convenient to choose a time step $\Delta t = 1/R_5$, consequently adatoms will perform, on average, one hop per time step. The hopping probability Γ will be therefore given by

$$\Gamma = \begin{cases} 1 & \text{if } N_b \leq 5, \\ \min(1, \tilde{\Gamma}) & \text{if } N_b > 5, \end{cases} \quad (28)$$

where

$$\tilde{\Gamma} \equiv \exp([(5 - N_b)\gamma + \Delta E_s - \Delta E_0]/k_B T). \quad (29)$$

For realistic values of the parameters, the chances that $\tilde{\Gamma}$ is greater than 1 are rather low, and therefore we believe that (28) is a good approximation of the actual dynamics.

Finally, in order to reduce the number of rejections, we separate the lightly bonded ($N_b \leq 5$) and the more strongly bonded ($N_b > 5$) atoms in our implementation of kinetic Monte Carlo. This is done as follows. We take Q steps where we update the lightly bonded atoms and then take one step where the strongly bonded atoms are allowed to move. The accepted rate for the strongly bonded atoms is increased by a factor Q . The above discussion can be conveniently summarized by the following algorithm:

ALGORITHM

```

set  $n_{\text{Ehops}} = 0$ 
while  $k_{\text{step}} < N_{\text{step}}$  do
  ADATOM MOTION AND DEPOSITION
  for  $q = 1$  to  $Q$ 
    if  $(k_{\text{step}} \bmod N_{\text{add}} = 0)$ 
      choose a site a random and add an atom.
      Note: this sets the flux to  $F = 1/(\Delta t N_{\text{add}} M^2 a_s^2)$ 
    end if
    for  $k_{\text{atom}} = 1$  to  $M^2$ 
      • Choose a site at random among all  $M \times M$  sites (only atoms on the surface are allowed to move)
      • If there is germanium atom present compute  $N_b$  (number of bonds)
      • if  $N_b \leq 5$ 
        Let the atom hop
      end if
    end for
     $k_{\text{step}} = k_{\text{step}} + 1$ 
  end for
  ELASTIC RELAXATION
  ◦ Let the system come to mechanical equilibrium by solving Eq. (20) for the displacement field using the method outlined in Section 3.4
  BONDED ADATOM MOTION
  for  $k_{\text{atom}} = 1$  to  $M^2$ 
    If there is germanium atom present, compute  $N_b$ 
    if  $N_b > 5$ 
      • Compute a random number,  $r$  uniformly in  $[0,1]$ .
      • Use the displacement field to compute  $\Delta E_s$  (Eq. (26))
      • if  $r < Q \exp(-\gamma(N_b - 5) + \Delta E_s - \Delta E_0)/k_B T)$ 
        - perform a hop
        -  $n_{\text{Ehops}} = n_{\text{Ehops}} + 1$ 
        - if  $n_{\text{Ehops}} \bmod J = 0$ 
          Let the system come to mechanical equilibrium by solving Eq. (20)
        end if
      end if
    end if
  end for
end while

```

6. Numerical results

At the present time the algorithm is too slow to perform computations for realistic values of the parameters and observe effects due to elastic strain. For example, quantum dots observed in experiments are on the order of 20 nm. This would suggest that we should be computing on domains on the order of $100 \text{ nm} \times 100 \text{ nm}$, which, depending on the size of a_s , means computing on domains in the range of 256×256 to 1024×1024 . At the present time the largest domain for which we can simulate in a reasonable time is 64×64 . Since elastic phenomena are a bulk effect, then we have to increase the spring constants to be unphysically large in order to observe significant elastic interaction. In our simulations we choose $k_L a_s^2 / k_B T = 500$ and $k_D a_s^2 / k_B T = 250$. These values are significantly larger than physical values. For this choice of spring constants we can numerically compute the elastic energy of an adatom on an empty substrate; the results of these computations can be sum-

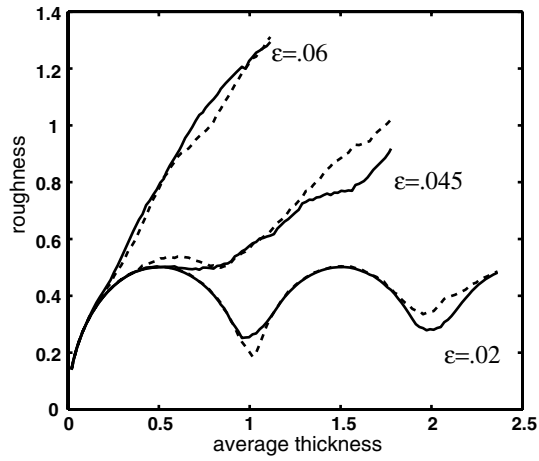


Fig. 4. Assessment of the KMC approximations. The roughness is plotted as function of average film thickness for different values of the misfit. The dotted lines are for $J = 8$ and $Q = 5$ whereas the solid line is for $J = 1$ and $Q = 1$.

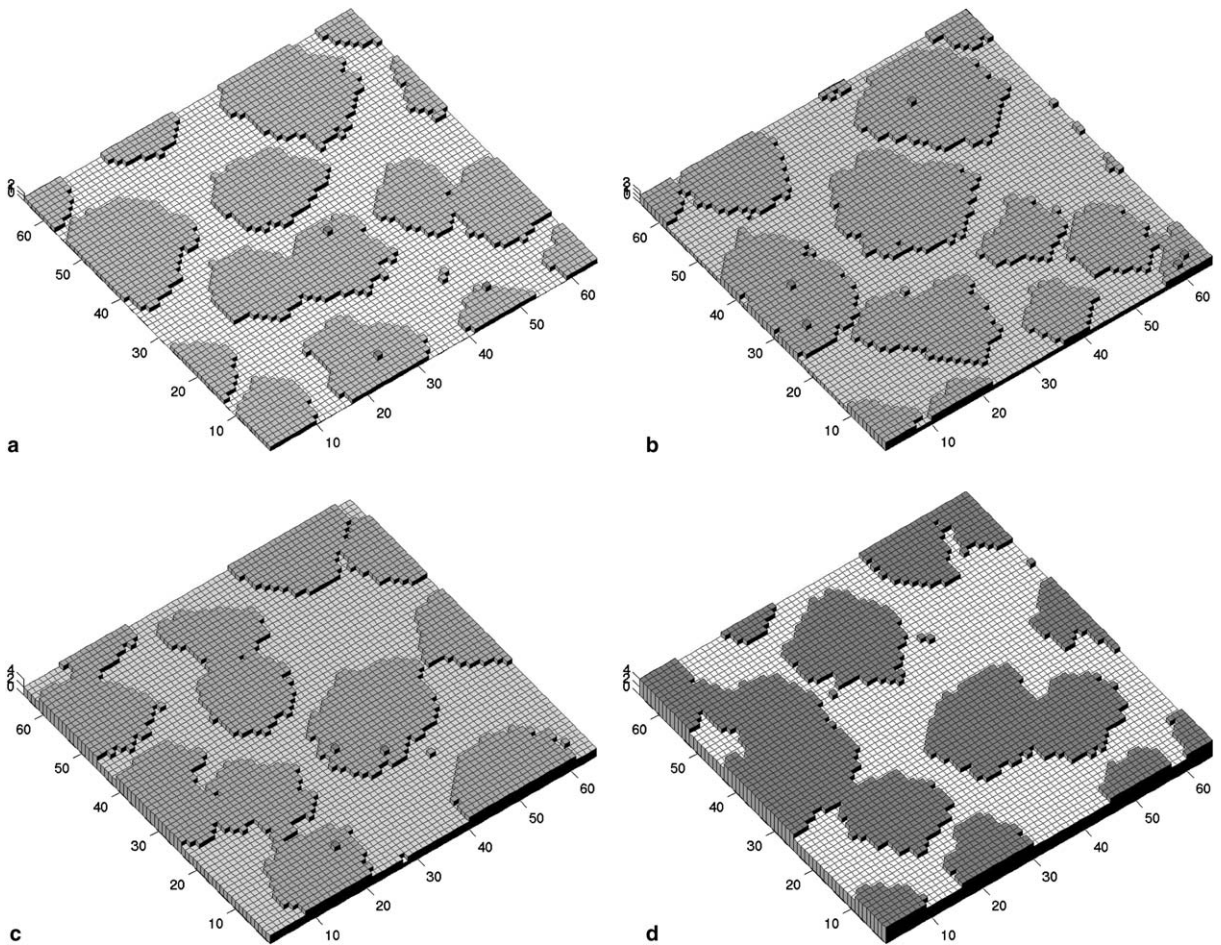


Fig. 5. Heteroepitaxial simulations with $\epsilon = 0.02$, all other parameter values are given in the text. (a) 0.5 monolayers, (b) 1.5 monolayers, (c) 2.5 monolayers, and (d) 3.5 monolayers. The number of gray levels is equal to the number of exposed layers.

marized from the formula $\Delta E_0 \approx 360\epsilon^2 k_B T$. In addition we choose $\gamma/k_B T = 2$. Therefore, it follows from using (27) that $\Delta t = R_0^{-1} \exp(10 - 360\epsilon^2)$. In our simulations, we choose the deposition rate, $a_s^2 \Delta t F = 10^{-5}$. Given the choice of our time step, the hopping rate for an adatom is unity and it follows that the diffusion coefficient is $D = a_s^2 / (4\Delta t)$. Consequently, we have $D / (a_s^4 F) = 2.5 \times 10^4$, which is a realistic deposition rate. Experimental values range between few hundreds to about 10^7 .

Finally, we have used $Q = 5$ and $J = 8$ for our approximation. These values have been determined as follows. Q is supposed to be the largest integer for which the quantity $Q \exp(-\gamma + \Delta E_s - \Delta E_0)$ very rarely exceeds 1. J is chosen in such a way that the mutual distance between atoms that have hopped is, on average, large enough not to influence the value of the local elastic energy. Such a value of J roughly scales with area of our substrate, M^2 . Numerical experiments revealed that taking smaller values for Q and J did not change the answer appreciably. For the simulations presented we have found that this choice of Q and J provided a significant increase in the computational speed over the $Q = 1$ and $J = 1$ case.

To assess the validity of the approximation, we computed the roughness of the film as a function of average film thickness, using $Q = 5$, $J = 8$, and compared the results with a computation performed with $Q = 1$, $J = 1$. The roughness is defined as

$$\text{roughness} = \sqrt{\frac{1}{M^2} \sum_{i,j} (h_{ij} - \bar{h})^2},$$

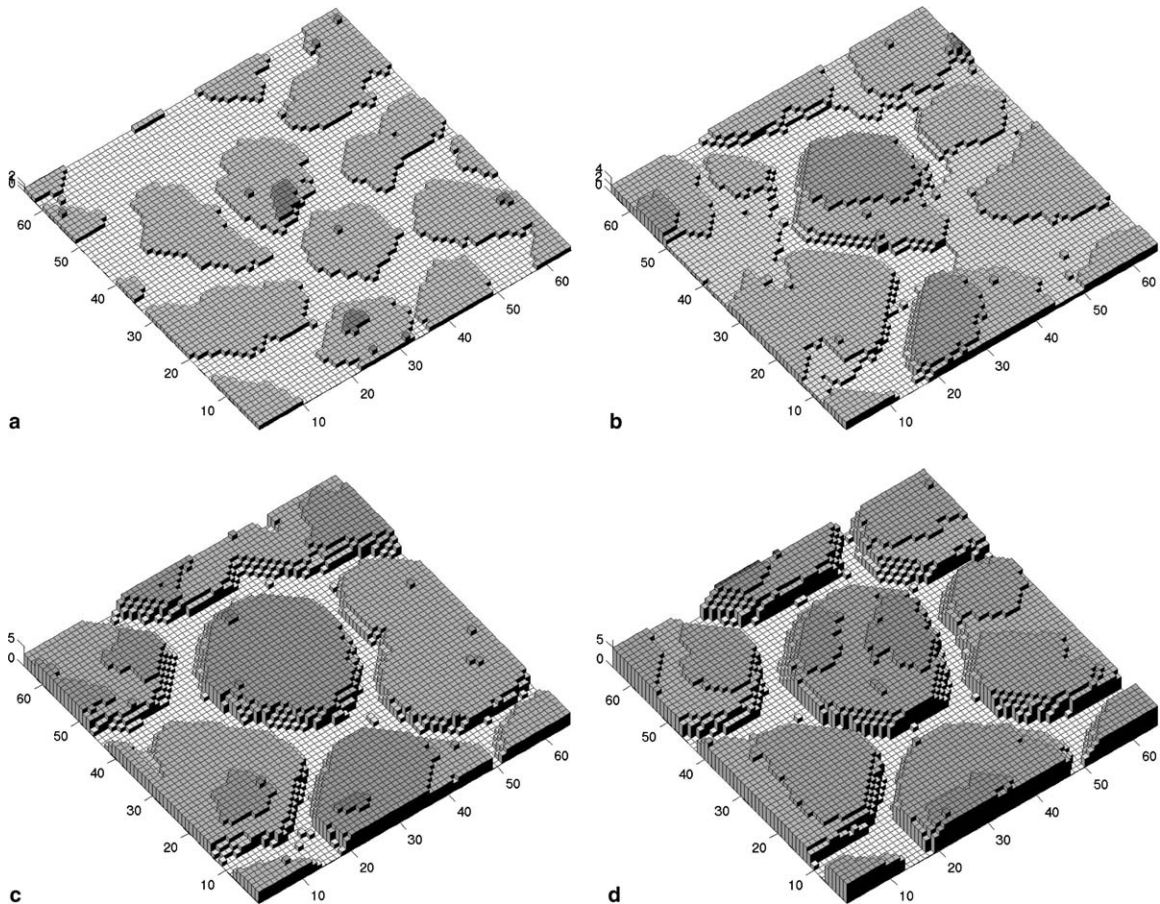


Fig. 6. Heteroepitaxial simulations with $\epsilon = 0.045$, all other parameter values are given in the text. (a) 0.5 monolayers, (b) 1.5 monolayers, (c) 2.5 monolayers, and (d) 3.5 monolayers. The number of gray levels is equal to the number of exposed layers.

where \bar{h} denotes the average height. The results, reported in Fig. 4, show a satisfactory agreement. For $\epsilon = 0.06$ the $Q = 5, J = 8$ case was 4.4 times faster than the case $Q = 1, J = 1$. For $\epsilon = 0.045$ it was 4.7 times faster and for $\epsilon = .02$ it was 3.5 times faster.

In Figs. 5–7, we present results of computations using the parameter values discussed above but we allow the misfit to vary. Fig. 5 shows the growth for $\epsilon = 0.02$. Here one observes layer-by-layer growth. Fig. 6 presents the results when $\epsilon = 0.045$. One observes that in the initial stages of growth the morphology is similar to layer-by-layer growth but three dimensional islands form by nucleation type events and by the formation of trenches [24]. The results for the case $\epsilon = 0.06$ are shown in Fig. 7. In this situation, three dimensional islands form very quickly by nucleation. The computations were performed on a Sun Blade 150 workstation, using f77 with -fast option. The CPU time was 21 h for $\epsilon = 0.02$, 78 h for $\epsilon = 0.045$, and 72 h for $\epsilon = 0.06$. All computations were performed using the approximation $Q = 5, J = 8$.

In both cases, $\epsilon = 0.045$ and $\epsilon = 0.06$, we observe Volmer–Weber growth. Simulations were performed over a wide range of parameter values and they always revealed a sharp transition between layer-by-layer growth and Volmer–Weber growth; Stranski–Krastanov growth was not observed. Our results are consistent with previous simulations [3,10,12,8,14,19] in this regard.

Fig. 8 summarizes a more extensive set of numerical simulations where the roughness of the film is evaluated when the average film thickness is 3.5 monolayers for misfit values between 0.01 and 0.06. This figure shows that there is a sharp transition from layer-by-layer to Volmer–Weber growth at a critical value of

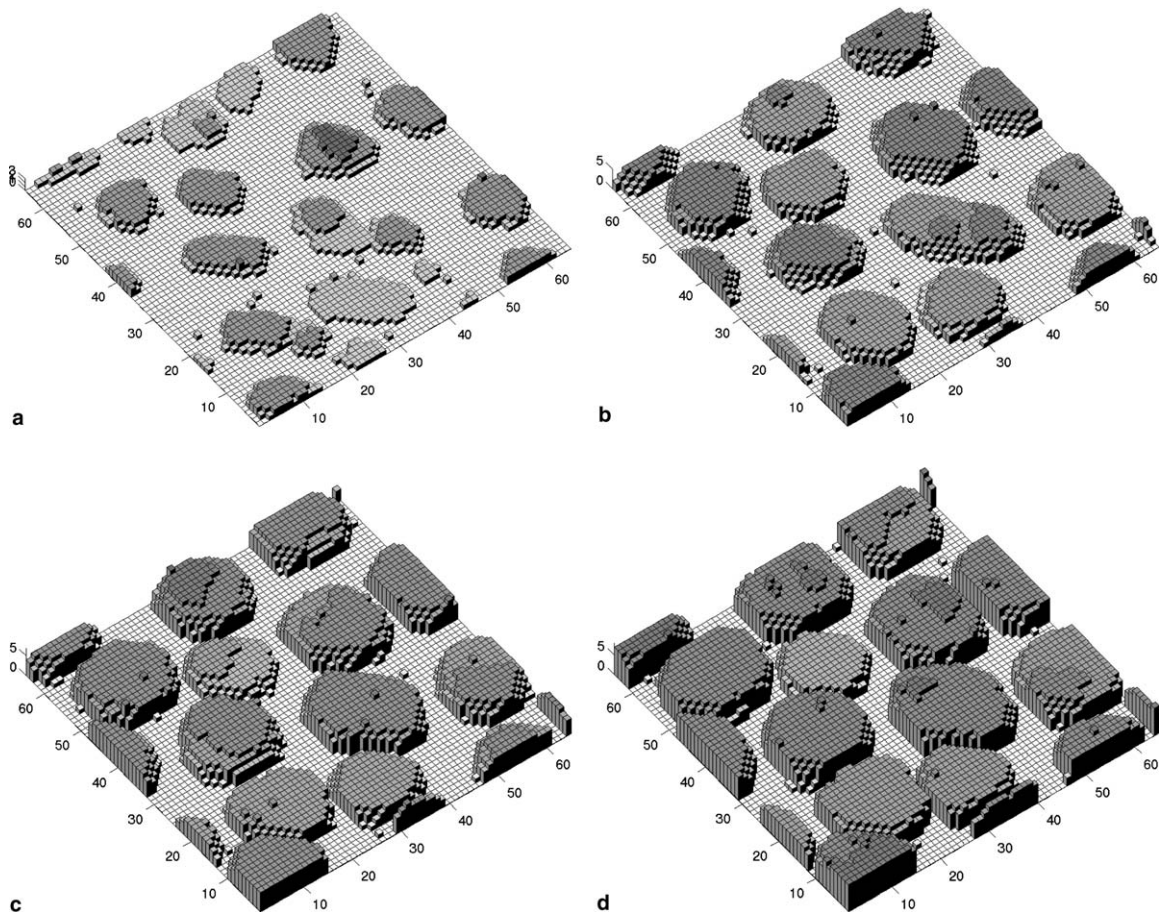


Fig. 7. Heteroepitaxial simulations with $\epsilon = 0.06$, all other parameter values are given in the text. (a) 0.5 monolayers, (b) 1.5 monolayers, (c) 2.5 monolayers, and (d) 3.5 monolayers. The number of gray levels is equal to the number of exposed layers.

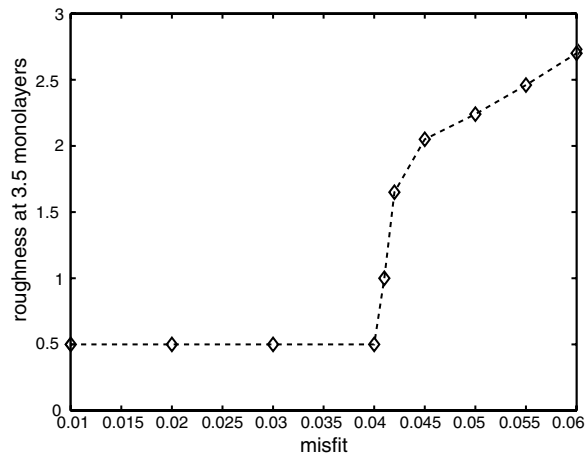


Fig. 8. The roughness when the average film thickness is 3.5 monolayers is plotted as function of the misfit. Each diamond represents the average of two simulations. The computations are performed on a 64×64 domain.

the misfit. This may be explained as follows: lowering ϵ increases the average island size; when the latter becomes too large, the islands cannot be represented on the domain, and layer-by-layer growth is observed. We speculate that, as size of domain tends to infinity, the critical misfit tends to zero.

7. Summary

A numerical method for the computation of heteroepitaxial growth (say germanium on silicon) in the presence of strain using kinetic Monte Carlo has been presented. A solid-on-solid model is used and the elastic effects are incorporated using a linear ball and spring model, and it is assumed that the structure is in mechanical equilibrium. This assumption allowed us to deduce an exact relation between the displacement field of the top layer of silicon atoms and the forces they generate, similar to a Dirichlet to Neumann map, which can be efficiently evaluated using a fast Fourier transform. Consequently, the resulting large linear system for the displacement field has only germanium atoms and one layer of silicon atoms as unknowns. The forces generated by the germanium atoms can be efficiently evaluated directly since the matrices that govern these interactions are sparse due to the fact the interactions are only between nearest and next nearest neighbors. The resulting system is solved iteratively using the conjugate gradient method. Finally, we introduce various approximations in the implementation of the KMC to improve the computation speed. Numerical results show that layer-by-layer growth is unstable if the misfit is large enough resulting in the formation of three dimensional islands. Our results are in agreement with previous studies [3,10,12,8,14,19].

Currently, we are in the process of solving the elastic equations for the deposited atoms using multigrid and then coupling the multigrid solver to the exact solution in the substrate. In addition we plan to extend the model to allow for the deposition of several different atomic species.

Acknowledgments

The authors thank Len Sander for many useful conversations. The authors also thank Russel Caflisch and Christian Ratsch for helpful remarks; in particular for comments that ultimately lead to the approximation given by Eq. (26). PS was supported, in part, by NSF Grants DMS-0207402, DMS-0244419 and DMS-0509124. G.R. was supported by a grant from the Michigan Center for Theoretical Physics and grant from the Italian Government (PRIN project 2003, prot.n.2003011441_004).

Appendix A

In this appendix, we give the explicit expression of the force acting on silicon atoms.

A.1. Forces inside the substrate

$$\begin{aligned}
 f_{\ell j k} = & k_L(u_{\ell+1, j k} - 2u_{\ell j k} + u_{\ell-1, j k}) + \frac{k_D}{2}(u_{\ell+1, j k+1} + u_{\ell-1, j k+1} + u_{\ell+1, j k-1} \\
 & + u_{\ell-1, j k-1} + u_{\ell+1, j+1, k} + u_{\ell-1, j+1, k} + u_{\ell+1, j-1, k} + u_{\ell-1, j-1, k} - 8u_{\ell j k}) + \frac{k_D}{2}(v_{\ell+1, j+1, k} + v_{\ell-1, j-1, k} - v_{\ell+1, j-1, k} - v_{\ell-1, j+1, k}) \\
 & + \frac{k_D}{2}(w_{\ell+1, j k+1} + w_{\ell-1, j k-1} - w_{\ell+1, j k-1} - w_{\ell-1, j k+1}), \quad (30)
 \end{aligned}$$

$$\begin{aligned}
 g_{\ell j k} = & k_L(v_{\ell j+1, k} - 2v_{\ell j k} + v_{\ell j-1, k}) + \frac{k_D}{2}(v_{\ell j+1, k+1} + v_{\ell j-1, k+1} + v_{\ell j+1, k-1} + v_{\ell j-1, k-1} \\
 & + v_{\ell+1, j+1, k} + v_{\ell-1, j+1, k} + v_{\ell+1, j-1, k} + v_{\ell-1, j-1, k} - 8v_{\ell j k}) + \frac{k_D}{2}(u_{\ell+1, j+1, k} + u_{\ell-1, j-1, k} - u_{\ell+1, j-1, k} - u_{\ell-1, j+1, k}) \\
 & + \frac{k_D}{2}(w_{\ell j+1, k+1} + w_{\ell j-1, k-1} - w_{\ell j+1, k-1} - w_{\ell j-1, k+1}), \quad (31)
 \end{aligned}$$

$$\begin{aligned}
 h_{\ell j k} = & k_L(w_{\ell j k+1} - 2w_{\ell j k} + w_{\ell j k-1}) + \frac{k_D}{2}(w_{\ell j+1, k+1} + w_{\ell j+1, k-1} + w_{\ell j-1, k+1} + w_{\ell j-1, k-1} \\
 & + w_{\ell+1, j k+1} + w_{\ell-1, j k+1} + w_{\ell+1, j k-1} + w_{\ell-1, j k-1} - 8w_{\ell j k}) + \frac{k_D}{2}(u_{\ell+1, j k+1} + u_{\ell-1, j k-1} - u_{\ell+1, j k-1} - u_{\ell-1, j k+1}) \\
 & + \frac{k_D}{2}(v_{\ell j+1, k+1} + v_{\ell j-1, k-1} - v_{\ell j+1, k-1} - v_{\ell j-1, k+1}). \quad (32)
 \end{aligned}$$

A.2. Forces acting on each atom of the first layer of the substrate due to the other silicon atoms

$$\begin{aligned}
 f_{\ell j 0} = & k_L(u_{\ell+1, j, 0} - 2u_{\ell j, 0} + u_{\ell-1, j, 0}) + \frac{k_D}{2}(u_{\ell+1, j, -1} + u_{\ell-1, j, -1} + u_{\ell+1, j+1, 0} + u_{\ell-1, j+1, 0} \\
 & + u_{\ell+1, j-1, 0} + u_{\ell-1, j-1, 0} - 6u_{\ell j, 0}) + \frac{k_D}{2}(v_{\ell+1, j+1, 0} + v_{\ell-1, j-1, 0} - v_{\ell+1, j-1, 0} - v_{\ell-1, j+1, 0}) \\
 & + \frac{k_D}{2}(w_{\ell-1, j, -1} - w_{\ell+1, j, -1}), \quad (33)
 \end{aligned}$$

$$\begin{aligned}
 g_{\ell j 0} = & k_L(v_{\ell j+1, 0} - 2v_{\ell j, 0} + v_{\ell j-1, 0}) + \frac{k_D}{2}(v_{\ell+1, j+1, 0} + v_{\ell-1, j+1, 0} + v_{\ell+1, j-1, 0} + v_{\ell-1, j-1, 0} \\
 & + v_{\ell j+1, -1} + v_{\ell j-1, -1} - 6v_{\ell j, 0}) + \frac{k_D}{2}(u_{\ell+1, j+1, 0} + u_{\ell-1, j-1, 0} - u_{\ell+1, j-1, 0} - u_{\ell-1, j+1, 0}) \\
 & + \frac{k_D}{2}(w_{\ell j-1, -1} - w_{\ell j+1, -1}), \quad (34)
 \end{aligned}$$

$$\begin{aligned}
 h_{\ell j 0} = & k_L(w_{\ell j, -1} - w_{\ell j, 0}) + \frac{k_D}{2}(w_{\ell+1, j, -1} + w_{\ell-1, j, -1} + w_{\ell j+1, -1} + w_{\ell j-1, -1} - 4w_{\ell j, 0}) \\
 & + \frac{k_D}{2}(u_{\ell-1, j, -1} - u_{\ell+1, j, -1}) + \frac{k_D}{2}(v_{\ell j-1, -1} - v_{\ell j+1, -1}). \quad (35)
 \end{aligned}$$

References

- [1] The FFTW package was developed at MIT by Matteo Frigo and Steven G. Johnson. Informations can be found at the site <http://www.fftw.org/>.
- [2] J.G. Amar, F. Family, Mound formation, coarsening and instabilities in epitaxial growth, *Surf. Rev. Lett.* 5 (1998) 851–864.
- [3] M. Biehl, M. Ahr, W. Kinzel, F. Much, Kinetic Monte Carlo simulations of heteroepitaxial growth, *Thin Solid Films* 428 (2003) 52–55.

- [4] A.B. Bortz, M.K. Kalos, J.L. Lebowitz, New algorithm for Monte-Carlo simulation of Ising spin systems, *J. Comput. Phys.* 17 (1975) 10–18.
- [5] W.K. Burton, N. Cabrera, F.C. Frank, The growth of crystals and the equilibrium structure of their surfaces, *Trans. R. Soc. Lond. Ser. A* 243 (1951) 299–358.
- [6] M.D. Johnson, C. Orme, A.W. Hunt, D. Graff, J. Sudijono, L.M. Sander, B.G. Orr, Stable and unstable growth in molecular beam epitaxy, *Phys. Rev. Lett.* 72 (1994) 116–119.
- [7] J. Krug, P. Politi, T. Michely, Island nucleation in the presence of step-edge barriers: theory and applications, *Phys. Rev. B* 61 (2000) 14037.
- [8] C.H. Lam, C.K. Lee, L.M. Sander, Competing roughening mechanisms in strained heteroepitaxy: a fast kinetic Monte Carlo study, *Phys. Rev. Lett.* 89 (1–4) (2002) 16102.
- [9] M.T. Lung, C.-H. Lam, L.M. Sander, Island, pit and groove formation in strained heteroepitaxy, preprint.
- [10] F. Much, M. Ahr, M. Biehl, W. Kinzel, A kinetic Monte Carlo method for the simulation of heteroepitaxial growth, *Comput. Phys. Commun.* 147 (2002) 226–229.
- [11] A. Hilliges, C. Mehl, V. Mehrmann, On the solution of palindromic eigenvalue problems, in: *Proceedings of the European Congress on Computational Methods in Applied Sciences and Engineering*, Jyväskylä, July 24–28, 2004.
- [12] F. Much, M. Biehl, Simulation of wetting-layer and island formation in heteroepitaxial growth, *Europhys. Lett.* 63 (2003) 14–20.
- [13] M.E.J. Newman, G.T. Barkema, *Monte Carlo Methods in Statistical Physics*, Oxford University Press, New York, 1999.
- [14] B.G. Orr, D.A. Kessler, C.W. Snyder, L.M. Sander, A model for strain-induced roughening and coherent island growth, *Europhys. Lett.* 19 (1992) 33–38.
- [15] P. Politi, G. Grenet, A. Marty, A. Ponchet, J. Villain, Instabilities in crystal growth by atomic or molecular beams, *Phys. Rep.* 324 (2000) 271.
- [16] C. Ratsch, M.C. Wheeler, M.F. Gyure, Roughening due to edge diffusion for irreversible aggregation, *Phys. Rev. B* 62 (2000) 12636.
- [17] C. Ratsch, A. Zangwill, P. Šmilauer, Scaling of heteroepitaxial island sizes, *Surf. Sci. Lett.* 314 (1994) L937–L942.
- [18] C. Ratsch, A. Zangwill, Equilibrium theory of the Stranski–Krastanov epitaxial morphology, *Surf. Sci.* 293 (1993) 123–131.
- [19] C. Ratsch, P. Šmilauer, D.D. Vvedensky, A. Zangwill, Mechanism for coherent island formation during heteroepitaxy, *J. Phys. I France* 6 (1996) 575–581.
- [20] J.M. Rickman, D.J. Srolovitz, Defect interactions on solid surfaces, *Surf. Sci.* 284 (1993) 211–221.
- [21] A.C. Schindler, M.F. Gyure, G.D. Simms, D.D. Vvedensky, R.E. Caffisch, C. Connell, E. Lou, Theory of strain relaxation in heteroepitaxial systems, *Phys. Rev. B* 67 (2003) 075316.
- [22] V.A. Shchukin, D. Bimberg, Spontaneous ordering of nanostructure on crystal surfaces, *Rev. Mod. Phys.* 71 (1999) 1125.
- [23] M. Schroeder, D.E. Wolf, Diffusion on strained surfaces, *Surf. Sci.* 375 (1997) 129–140.
- [24] J. Tersoff, F.K. LeGoues, Competing relaxation mechanisms in strained layers, *Phys. Rev. Lett.* 72 (1994) 3570.